An application-specific design approach for 2D ultrasonic arrays.

Jerzy Dziewierz, Anthony Gachagan
Centre for Ultrasonic Engineering,
Jerzy.Dziewierz@eee.strath.ac.uk

Natacha Lord, Anthony J. Mullholland
Department of Mathematics and Statistics,

University of Strathclyde, Glasgow, UK
Jerzy.Dziewierz@eee.strath.ac.uk

Abstract

As the technology of 2D phased array probes develops in the direction of sparse location of the elements, developing a balance of image resolution, contrast, coverage, and cost of the system becomes essential. A software-hardware system has been built that allows estimating 3D coverage of the inspection with respect to image quality for a given probe design. GP-GPU implementation of the algorithms enables calculations to be performed in a practical timeframe.

1. Introduction

2D phased ultrasonic arrays offer reduced inspection time and cost through collecting more information from a single location, when compared to 1D phased arrays. In some inspection scenarios, mechanical scanning might become unnecessary. Development of these promising probes currently goes into direction of sparse random location of array elements [1][2][3][4][5], that is, irregular or aperiodic location of elements over the aperture of the probe, where the median distance between the elements is much larger than half of the dominant wavelength of the ultrasonic pulse in the load media. This dramatically lowers the cost of the probe and related instrumentation when compared to a 'fully sampled' probe. Such approach is being combined with advanced signal processing algorithms to produce 2D and 3D images that are comparable to their ‘dense’ matrix probe counterparts, and useable for purposes of the inspection.

In order to achieve the required ultrasonic image quality at lowest possible system cost, there remains a need to design the probe elements, their configuration, overall probe aperture, bandwidth and other characteristics, taking into account properties of the novel imaging algorithms. Traditional, beam-shape modelling methods are insufficient as they often neglect contrast improving features of the new algorithms. In fact, the main factor deciding on the suitability of a given inspection method for a given inspection scenario, is image contrast, defined here as the distinguishable difference between actual defects and image clutter. Additionally, if the image is of high spatial resolution, more detailed characterisation of the defect can be obtained. It should be noted that contrast, resolution, and sensitivity of the image has to be traded against the cost of the probe in the probe design stage.

2. The cuMAP software package

cuMAP is a software suite that simulates full pulse-echo and pitch-catch imaging performance of the entire 3D imaging system, across a volume of interest. This package takes into account probe properties, imaging algorithm properties and load material properties. Sensitivity, coverage, and most importantly, contrast of the image offered by the system of given design can be estimated before building the probe. The specimen material can be multi-layered, and curved interfaces (eg. pipes or nozzles) are supported. In order to perform calculations in a practical time frame, performance-critical sections have been implemented using emerging GP-GPU technology in NVIDIA CUDA framework[6].

3. Methodology

The simulation process is illustrated in Fig. 1. Firstly, the Phased Array Controller (PAC), probe, specimen, and imaging algorithm description is collated into a database. Next, the imaging volume of interest inside the specimen is defined. For each imaging point inside the specimen (voxel, volume picture element), a simulated, point-like reflector is created and the FMC (Full Matrix Capture) data simulated as transmitted and received using the previously described probe/PAC/specimen combination. An image of this reflector is obtained using the selected advanced imaging algorithm, which might be executed on the GPU for performance. This image is a "point spread function" for a given location. This image is then analysed automatically and image quality characteristics extracted. Currently four parameters are recorded: relative sensitivity, -3dB spot size, side lobe level, and leakage factor. These image quality characteristics can be described as follows:

- **Spot size** – represents the main lobe size at the reflector location, since the reflector itself is point-like. This corresponds to imaging resolution (smallest distance between two distinguishable reflectors) and should not be confused with the smallest detectable reflector.
- **Maximum side lobe level** – corresponds to the maximum amplitude of a lobe that is not connected to the main lobe. This corresponds to a worst case imaging artefact – showing a reflector where there isn't one, but the suspected region is close to other strong reflectors. One can relate this to false positive rate of detection.
- **Signal Leakage** – integral of the image energy outside the main lobe. This corresponds to worst imaging artefact when trying to detect a lack of reflection, close to other reflectors. One can relate this to false negative rate of detection.
- **Relative signal sensitivity** - for arrays with directional elements, sensitivity drops drastically for off-axis reflectors. Sensitivity also falls for reflectors that are far away from an array with omnidirectional elements. This measure can be related to smallest detectable reflector.

Spot size is indicative of actual resolution of the image, while side lobe level and leakage factor indicate image contrast. Relative sensitivity is important to establish coverage of the imaging system, since there might be places where ultrasonic energy does not reach. An example reason might be that the probe's elements are directional, or the refraction angle is too shallow. Currently, no complex geometry effects such as shadows or re-radiating surface

waves are simulated; however, curved material interfaces that refract sound are taken into account.

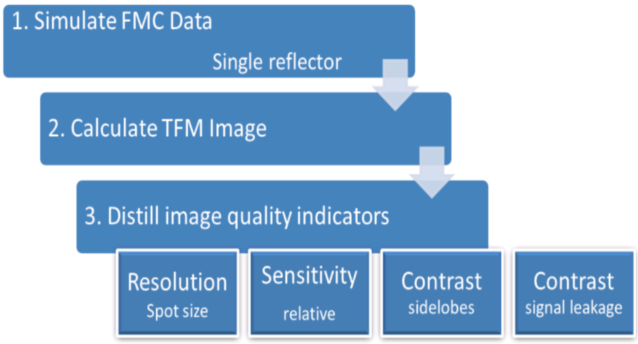

Figure 1. the cuMAP process - per pixel

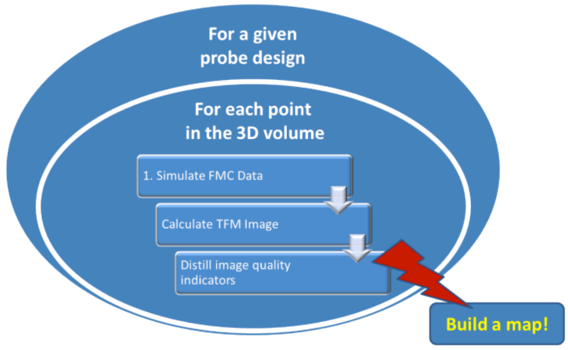

Figure 2. cuMAP process - overview

4. The Full Matrix Capture simulation module

A computationally inexpensive method of obtaining simulated FMC data was created for this work. For simplicity, only point like reflectors and hard fixed surface reflectors are supported in the module. Furthermore, a simplifying assumption has been made that the temporal shape of the reflected signal is the same irrespective of location and distance to the reflector. Directivity of the probe's element and propagation distance is taken into account as a reduction in amplitude of the returned signal.

The FMC simulation module works as follows. A recording of the pulse-echo signal has been obtained using single element of the phased array of interest. Directivity of the probe element has been modelled using raised cosine function:

$$y(\alpha) = \cos(\alpha)^{\beta} \quad \text{(1)}$$

Where 'y' is a fraction (reduction of) of amplitude at given α; α is angle formed between axis of the array element and the line leading from the array element to the reflector; and β is a experimentally-measured parameter of directivity. The parameter has been obtained using curve fit to the measured amplitude of return signal in an experiment where a moving reflector has been presented to the probe.

The FMC simulation works by inserting the measured pulse-echo signal, (with amplitude modified by the element directivity model and distance), into the FMC matrix at a position that is dictated by the calculated time of propagation between the transmitting element, reflector and the receiving element. Refraction through layered media is taken into account, and the interface can be curved. All other effects are ignored. Strength of the reflector can be modified to simulate effects of shadowing of small reflectors by side lobes of larger reflectors.

Such method yields a simple, computationally cheap computer program that generates FMC data amenable to imaging using standard or novel ultrasonic imaging algorithms. Additionally, the algorithm is easily parallelisable for execution on multicore or GPU systems for extra performance, as individual lines of the FMC are essentially computationally independent.

5. Experimental validation

To validate the program and estimate the combined effect of simplifications assumed in the algorithm, the following experiment has been performed.

FMC data has been experimentally acquired, using a ZETEC Dynaray PA Controller, for a φ5mm steel sphere reflector suspended in water, as illustrated in Fig. 3. It is acknowledged that this reflector is not an ideal point-like reflector, but only a coarse approximation of one.

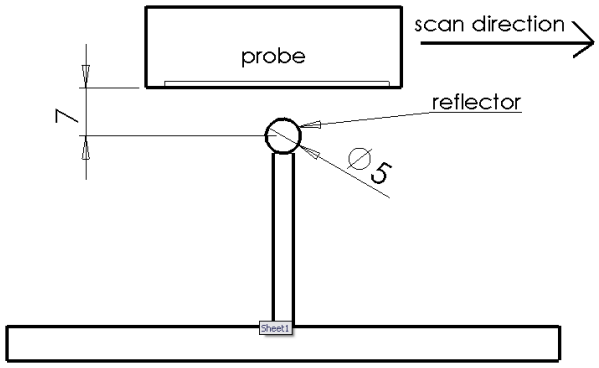

Figure 3. Experimental setup - side view

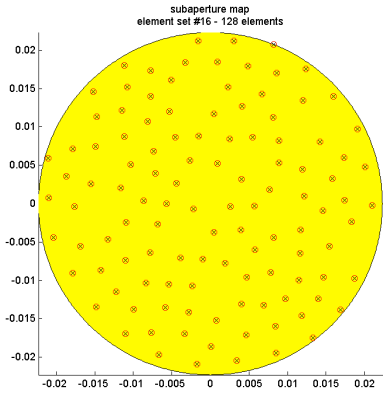

Figure 4. Location of array elements in the probe's aperture (element sizes not to scale)

In order to simulate a number of varied "virtual probes", subapertures of the actual probe have been used for imaging. Fig. 4 illustrates the 128 element sparse array configuration utilised in this work and 16 subapertures of varied element counts have been selected. Using these subapertures, simulated and experimental data has been used to obtain image of the reflector, and the images have been compared. The basic characteristics of the image have been extracted and are presented in Fig 5.

Comparison of measured and simulated size of the main spot in the image, -3dB diameter

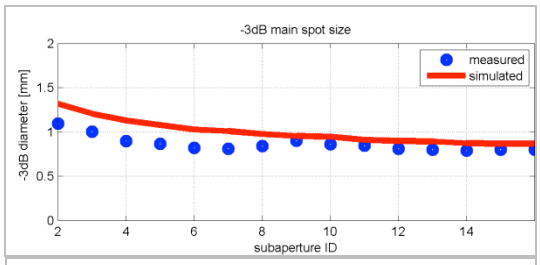

Comparison of measured and simulated size of the main spot in the image, -6dB diameter

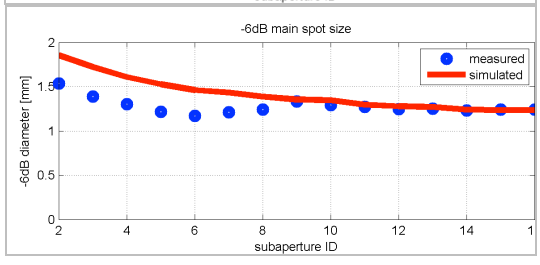

Comparison of measured and simulated amplitude of the sidelobe

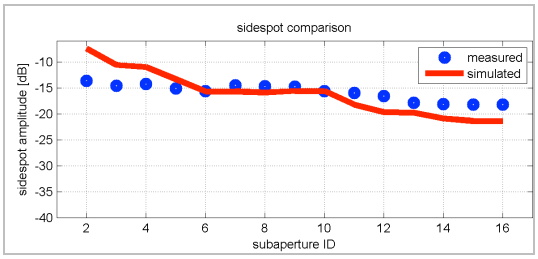

Fig 5. Comparison between simulated and experimental array performance parameters

In most cases, the resolution of the image is underestimated (spot size overestimated). Such error is considered to be on the "safe side" as a manufactured array design will exceed the performance of the simulation. This has occurred because the template pulse-echo signal that has been selected for use in the simulation has been selected from among the worst of the probe's elements (longest ring down time).

The side spot amplitude for the larger apertures becomes underestimated and this can be explained by the fact that with the larger aperture, the secondary reflections coming from the support rig impinge on the image of the reflector of interest, increasing "apparent noise" of the measured image.

The "uneven" descent of the simulated side spot amplitude against sub-aperture index is a result of the quasi-random "Poisson disk" distribution of the array elements. The contribution of individual elements to the reduction of the side spot amplitude varies depending on its location relative to the reflector; hence the observed effect. It is worthwhile noting that the trends of measured and simulated results have their breaking points in the very same locations.

The simulation results are within +-20% of the experimental results, and general trends are preserved. It is concluded that such error is acceptable for current simulation needs. Depending on the application, a more precise way might be implemented by taking into account some of the neglected effects. It is proposed that should the need arise, the next best candidate effect for simulation is the variation of frequency content (and shape) of the received pulse with angle of its arrival into the probe.

6. GP-GPU implementation of the 3D Total Focussing Method algorithm

For purpose of this work, the Total Focussing Method (TFM) imaging algorithm[7] has been implemented using NVIDIA CUDA. The TFM algorithm is a great candidate for parallel implementation because of its high overall computational cost, easy parallelisation, and high quality resulting image. In this algorithm for each pixel of the image, for each transmitter-receiver combination, a propagation delay has to be calculated, and appropriate data sample from the FMC accumulated into the pixel to form the image. For example, for a 128 element probe, 240x240x320 pixel image, 240*240*320*128*128*0.5 ≈ 151e9 delays have to be calculated. The 0.5x factor is because for each probe element pair, the propagation delay is the same if any of the elements acts as receiver.

Details of this work are outside of the scope of this paper. However, it is worth noting that the current implementation supports refraction through curved surfaces and achieves performance of approximately 2300e6 delays/second on a single NVIDIA GTX580 GPU. The algorithm easily expands to multiple GPUs and parallel operation across 8 GPUs has been demonstrated, with a small overhead for starting the parallel job and downloading the results. This means that the image for the 128 element example described in the previous paragraph can be obtained in under 12 seconds. Moreover, it is expected that the process can be accelerated to 'real time interactive' standard with additional computing resources.

7. Example map of resolution and contrast

An example, 3MHz, 128 element, sparse 2D phased array probe has been analysed using cuMAP software. Maps of resolution, contrast and sensitivity have been obtained for a 2D slice through volume of water in which the probe is immersed. The slice has dimensions 15mm x 35mm and has been sampled in a regular grid of 2mm in each direction. Full aperture of the probe has been used for both transmission and reception and the imaging algorithm is Total Focussing Method.

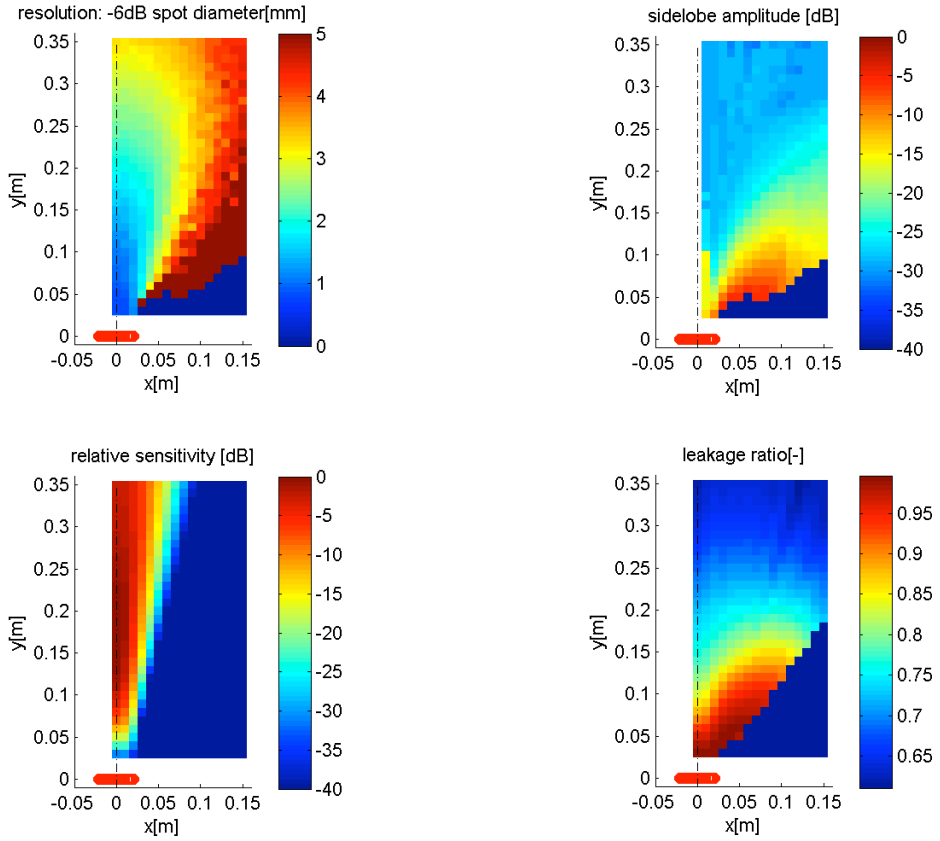

Figure 6. Calculated image quality maps - example

The maps reproduced in Fig. 6 describe variation of the calculated image quality across the volume. If the required image quality is well defined for a given inspection scenario, a combined map of coverage of the inspection can be obtained as depicted in Fig 7. To produce this Figure, the following design criteria has been assumed: sensitivity >-30dB of peak, spot size Ø<2mm, side lobe amplitude <-20dB. It can be noted that regular Total Focussing Method (TFM) does not produce best results in the area directly below the probe. This is not the limitation of TFM, but rather the probe itself: the limiting factor is reduction of sensitivity due to directivity of elements, where some of the elements do not 'see' the test reflector placed at that location. It is proposed that a sub aperture TFM imaging could be used in that area to resolve the situation.

Apparent 'noisiness' of the maps is a result of finite discretisation of the TFM images, resulting in quantisation error of measurement of simulated image features.

8. Conclusions

The presented approach will be used to design 2D phased array probes that fully match NDE inspection scenario requirements, while minimising the cost of both probe and related data acquisition and processing system. Main feature distinguishing cuMAP from other similar systems is that properties of the imaging algorithms are taken into account, and the calculations are arranged in way that allows utilisation of massively parallel computers, completing calculations in practical timeframe.

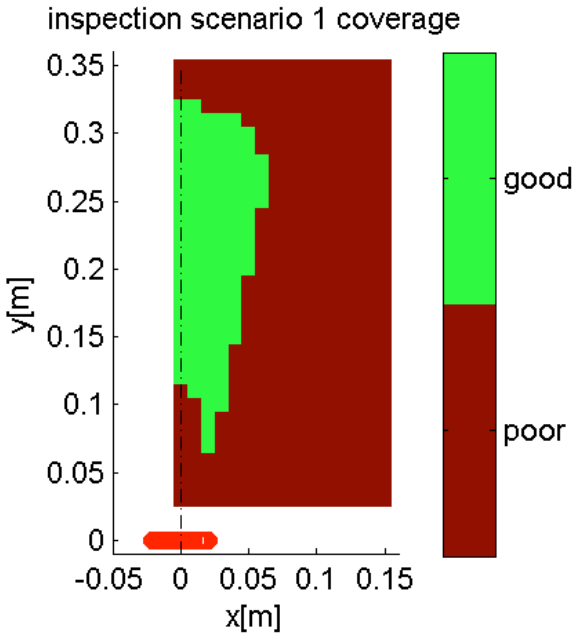

Figure 7. Map of acceptable quality of image assuming example inspection requirements.

Acknowledgements

The authors would like to acknowledge EPSRC (EP/H001387/1) for providing financial support for this work and our industrial partners, Rolls Royce, for guidance on the development of this design approach.

References

1. O. Martínez-Graullera, C. J. Martín, G. Godoy, and L. G. Ullate, '2D array design based on Fermat spiral for ultrasound imaging', *Ultrasonics*, vol. 50, no. 2, pp. 280–289, 2010.
2. S. N. Ramadas, J. C. Jackson, A. Tweedie, R. L. O'Leary, and A. Gachagan, 'Conformally mapped 2D ultrasonic array structure for NDT imaging application', in *Ultrasonics Symposium (IUS), 2010 IEEE*, 2010, pp. 33 –36.
3. M. R. Bai, J.-H. Lin, and C.-W. Tseng, 'Implementation issues of the nearfield equivalent source imaging microphone array', *Journal of Sound and Vibration*, vol. 330, no. 3, pp. 545–558, Jan. 2011.
4. A. Tweedie, V. Murray, and G. Hayward, 'Aperiodic and deterministic 2D phased array structures for ultrasonic imaging', in *Ultrasonics Symposium (IUS), 2009 IEEE International*, 2009, pp. 406 – 409.

5. S. Mitra, K. Mondal, M. Tchobanou, and G. Dolecek, 'General polynomial factorization-based design of sparse periodic linear arrays', *IEEE Trans. Ultrason., Ferroelect., Freq. Contr.*, vol. 57, no. 9, pp. 1952–1966, Sep. 2010.
6. 'CUDA, Supercomputing for the Masses: Part 1 | Dr Dobb's'. [Online]. Available: http://drdobbs.com/architecture-and-design/207200659?pgno=2. [Accessed: 25-Sep-2011].
7. C. Holmes, B. Drinkwater, and P. Wilcox, 'The post-processing of ultrasonic array data using the total focusing method', *Insight - Non-Destructive Testing and Condition Monitoring*, vol. 46, no. 11, pp. 677–680, Nov. 2004.